GEOPHYSICS, VOL. 75, NO. 1 (JANUARY-FEBRUARY 2010); P. V1–V12, 12 FIGS., 2 TABLES.
10.1190/1.3294424

Implementation of 2D explicit depth extrapolation FIR digital filters for 3D seismic volumes using singular value decomposition

Wail A. Mousa[1], Said Boussakta[2], Desmond C. McLernon[3], and Mirko Van der Baan[4]

ABSTRACT

We propose a new scheme for implementing predesigned 2D complex-valued wavefield extrapolation finite impulse response (FIR) digital filters, which are used for extrapolating 3D seismic wavefields. The implementation is based on singular value decomposition (SVD) of quadrantally symmetric 2D FIR filters (extrapolators). To simplify the SVD computations for such a filter impulse response structure, we apply a special matrix transformation on the extrapolation FIR filter impulse responses where we guarantee the retention of their wavenumber phase response. Unlike the existing 2D FIR filter implementation methods that are used for this geophysical application such as the McClellan transformation or its improved version, this implementation via SVD results in perfect circularly symmetrical magnitude and phase wavenumber responses. In this paper, we also demonstrate that the SVD method can save (depending on the filter size) more than 23% of the number of multiplications per output sample and approximately 62% of the number of additions per output sample when compared to direct implementation with quadrantal symmetry via true 2D convolution. Finally, an application to extrapolation of a seismic impulse is shown to prove our theoretical conclusions.

INTRODUCTION

The frequency-space (or frequency-inline-crossline) ($\omega - x - y$) explicit depth wavefield extrapolation method is considered to be one of the most attractive techniques for performing 3D wavefield extrapolation (Holberg, 1988; Hale, 1991b; Karam and McClellan, 1997; Thorbecke, 1997;Yilmaz, 2001). The most important feature of such a technique is that it can be used for accurate migration of one-way wavefields through heterogeneous media. It also results in stable extrapolated wavefields because of new improvements in the design of these finite impulse response (FIR) digital filters, like the ones reported in Hale (1991b); Karam and McClellan (1995); Soubaras (1996); Thorbecke et al. (2004); and Mousa et al. (2005, 2006).

2D wavefield extrapolation finite impulse response (FIR) filters for extrapolating 3D seismic wavefields

Assuming that $\Delta x = \Delta y$, where Δx and Δy are respectively the inline and crossline spatial sampling intervals, the frequency-wavenumber response of the 3D extrapolation filter is given by (Yilmaz, 2001; Hale, 1991b; Karam and McClellan, 1997):

$$H_d(k_x,k_y,\omega) = \exp\left[j\frac{\Delta z}{\Delta x}\sqrt{\frac{\Delta x^2}{\Delta t^2}\frac{\omega^2}{c_o^2} - (k_x^2 + k_y^2)}\right], \quad (1)$$

where k_x and k_y are the normalized inline and the crossline wavenumbers, Δz is the extrapolation depth step size, Δt is the time-sampling interval, $\omega \in [-\pi, \pi]$ is the normalized angular frequency, c_o is the propagation velocity related to the geological material, and $j = \sqrt{-1}$. The explicit depth wavefield extrapolation for 3D seismic data sets is performed one frequency (ω) at a time using 2D migration filters $H_d(k_x,k_y)$:

$$H_d(k_x,k_y,\omega) = H_d(k_x,k_y) = \exp[jb\sqrt{k_{c_p}^2 - (k_x^2 + k_y^2)}], \quad (2)$$

where $b = \Delta z/\Delta x$ and $k_{c_p} = \frac{\Delta x}{\Delta t}\frac{\omega}{c_o}$ is the cutoff wavenumber. Equation 2 represents the desired 2D wavenumber response of our spatial filter where the magnitude and phase responses are of circular symmetry.

The $\omega - x - y$ extrapolation of a spatially sampled seismic wavefield $u(x_i,y_j,\omega,z_k)$ from depth say z_k to $z_{k+1} = z_k + \Delta z$ is performed independently for each frequency by a direct 2D spatial convolution with a designed 2D FIR filter impulse response $h[n_1,n_2]$ (approxi-

Manuscript received by the Editor 3 November 2008; revised manuscript received 22 June 2009; published online 12 February 2010.
[1]King Fahd University of Petroleum and Minerals, Department of Electrical Engineering, Dhahran, Saudi Arabia. E-mail: Wailmousa@kfum.edu.sa.
[2]Newcastle University, School of Electrical, Electronic and Computer Engineering, Newcastle upon Tyne, U. K. E-mail: S.Boussakta@ncl.ac.uk.
[3]The University of Leeds, School of Electronic & Electrical Engineering, Leeds, U. K. E-mail: D.C.McLernon@leeds.ac.uk.
[4]The University of Leeds, School of Earth and Environment, Leeds, U. K. E-mail: m.van-der-baan@see.leeds.ac.uk.

mating equation 2) using (Holberg, 1988; Hale, 1991b; Thorbecke, 1997):

$$u(x_i,y_j,\omega_\ell,z_{k+1}) = \sum_{n_1=(-N+1)/2}^{(N-1)/2} \sum_{n_2=(-N+1)/2}^{(N-1)/2} h[n_1,n_2] \times u(x_{i-n_1},y_{j-n_2},\omega_\ell,z_k), \quad (3)$$

where n_1 and n_2 stand for the inline and crossline spatial indices, and $h[n_1,n_2]$ is a quadrantally symmetric $N\times N$ (N odd) complex-valued 2D FIR impulse response, i.e.,

$$h[n_1,n_2] = h[-n_1,n_2] = h[n_1,-n_2] = h[-n_1,-n_2]. \quad (4)$$

In this case, the extrapolation (filtering) process is carried over all frequencies ω_ℓ, where $\ell = 0,\ldots,M-1$ and M is the number of frequency samples. A typical $\omega - x - y$ wavefield extrapolation process requires a set of 2D frequency-velocity-dependent complex-valued FIR filters that are designed and stored in a table for reuse to extrapolate the seismic wavefield from one depth level $u(x_i,y_j,\omega_\ell,z_k)$ to the next $u(x_i,y_j,\omega_\ell,z_{k+1})$. Let us assume that the number of samples in both spatial directions (say n_x and n_y) are equal to each other ($n_x = n_y = n_s$). Then for each frequency sample we require n_s^2 convolutions because the convolution extrapolation is performed at each spatial sample location. If, for example, we have 1000 frequency samples, then this results in performing $1000\times n_s^2$ 2D convolution processes to get only one depth slice of the final 3D extrapolated wavefield. So if one needs 500 depth slices, $500{,}000\times n_s^2$ 2D convolutions are required. Using direct convolution of these 2D complex-valued $N\times N$ impulse responses, the computational cost will be $500{,}000\times n_s^2\times N^2$, where N^2 is the FIR filter size in the spatial directions' indices n_1 and n_2. In this application, even by taking advantage of the quadrantally symmetric property of such 2D impulse responses, the computational effort will still be high (Reshef and Kessler, 1989; Yilmaz, 2001).

State of the art

Different approaches have been proposed to mitigate such a computationally expensive 3D extrapolation process that relies so heavily on direct convolution with a 2D complex-valued FIR filter impulse response (Thorbecke and Berkhout, 1994). One way to mitigate this problem is to design those 2D FIR extrapolators with small sizes (Soubaras, 1996; Thorbecke et al., 2004; Mousa et al., 2009). The other way is by finding means of implementing predesigned 1D or 2D FIR filters. The first approach, in the latter case, (known in the geophysics literature as splitting) is where the extrapolating is performed by splitting the process to alternately extrapolate along the inline and crossline directions, independently (Hale, 1991a), i.e., assuming that the 2D extrapolation FIR filters are separable. This method is cheap in the sense that its computational complexity is proportional to the used FIR filter length N and is based on the 2D Fourier transform approximation of the desired extrapolation wavenumber response. It will also result in stable extrapolated images. However, it results in large errors for wavenumber cutoffs in which $k_x \approx k_y \gg 0$. This corresponds to steep dipping at 45° azimuth between the inline and crossline directions (Hale, 1991a).

The second approach relies on the popular McClellan transformations where it uses Chebychev structures and is very suitable for 2D FIR filters with a quadrantal symmetry property, like our extrapolation filters (Mecklenbräuker and Mersereau, 1976; McClellan and Chan, 1977; Kayran and King, 1983; Dudgeon and Mersereau, 1984; Hale, 1991a; Lu and Antoniou, 1992; Karam and McClellan, 1997). Their cost is proportional to the filter length N, and 1D filters are needed to obtain the 2D FIR impulse response, based on a transformation filter (Hale, 1991a). The transformation will result in stable extrapolated images and is best for small wavenumbers — it is exact for $k_x = k_y = 0$ — but exhibits increasing error with increasing wavenumbers where $k_x \approx k_y$. An improved McClellan transformation filter was proposed by Hale (1991a) to overcome such wavenumber response errors where the transformation filter (matrix) is larger than the original one (see, for example, McClellan and Chan, 1977; Dudgeon and Mersereau, 1984), such that it results in a better approximation of the circularly symmetric property of the 2D migration wavenumber response as shown in equation 2. The computational complexity of this improved McClellan transformation filter is higher than the previous McClellan transformation, but it is still proportional to N (Hale, 1991a). None of these transformations, however, yield exactly circularly symmetric extrapolation wavenumber responses.

Problem definition: Revisited

Thus, there is a need for extrapolating 3D seismic data sets with true 2D extrapolation FIR filters that are cheap to implement, result in stable extrapolated wavefields, and better approximate circular symmetry with respect to their wavenumber responses. Digital FIR filter implementation techniques based on singular value decomposition (SVD) have been proposed for implementing 2D zero-phase real-valued FIR digital filters (Lu et al., 1990, 1991) and, more recently, for 2D linear-phase real-valued FIR digital filters (Zhu et al., 1999). In both papers, 2D FIR filters were predesigned and then implemented using the SVD technique for general FIR filters, including symmetrical and antisymmetrical ones. The SVD implementation structure has the following advantages:

- It is suitable for parallel processing such as the case for $\omega - x - y$ extrapolation.
- It is flexible in the sense that we can select the number of parallel sections that correspond to the most significant singular values. Hence, this results in savings in computational complexity at the expense of introducing small errors in the wavenumber response.
- Depending on the number of parallel sections used in the implementation, its computational complexity is proportional to the FIR filter's impulse response length N.

Application to wavefield extrapolation

In this work, we present the mathematical development of implementing 2D complex-valued quadrantally symmetric extrapolation FIR filters (for the $\omega - x - y$ 3D extrapolation) using SVD. To simplify the SVD computations for such an FIR filter impulse response structure (i.e., quadrantal symmetry), we apply a special matrix transformation similar to the one reported by Zhu et al., (1999) on the extrapolation filter impulse response, which guarantees that no distortion of the wavenumber phase response occurs and the magnitude responses will result in stable extrapolation. Also, this results in less numerical SVD computational errors. Additionally, we exploit the existence of insignificant singular values and discard them so we reduce the computational complexity of the expensive 3D $\omega - x - y$ extrapolation problem. As a result, our proposed implementa-

tion method for such application overcomes the problems of other previously reported and heavily used implementation schemes in terms of computational cost, stable extrapolated wavefields, and circularly symmetrical wavenumber response.

This paper is organized as follows. We start by introducing the concept of SVD implementation for 2D FIR digital filters. Also, we present the SVD implementation of 2D quadrantally symmetric complex-valued extrapolation FIR digital filters. Then, we elaborate on error analysis, relating to the SVD implementation of extrapolation filters. After that, we perform simulation results to evaluate the accuracy of the 2D extrapolation FIR filters implemented using our proposed SVD scheme. We also show impulse responses of our proposed method. We give a brief discussion afterward. Finally, we highlight the major contributions of this paper in the conclusion section.

SVD IMPLEMENTATION FOR 2D COMPLEX-VALUED EXTRAPOLATION FIR IMPULSE RESPONSE

Let $h[n_1,n_2]$ be an already designed $N\times N$ quadrantally symmetric 2D extrapolation FIR impulse response in the spatial domain, where $h[n_1,n_2]\in\mathbb{C}^{N\times N}$ for $n_1,n_2=-(N-1)/2,\ldots,(N-1)/2$ and N is an odd number. Define $\mathbf{A}$ to be an $N\times N$ matrix whose elements represent the quadrantally symmetric 2D extrapolation FIR impulse response as given by

$$\mathbf{A}=\{h[n_1,n_2]\},\quad \text{for } |n_1,n_2|\le(N-1)/2. \tag{5}$$

SVD and FIR implementation

In general, the SVD of $\mathbf{A}$ can be written as

$$\mathbf{A}=\mathbf{U}\boldsymbol{\Sigma}\mathbf{V}^*, \tag{6}$$

where $\mathbf{U}$ and $\mathbf{V}$ are unitary matrices, * denotes the complex conjugate transpose, and $\boldsymbol{\Sigma}$ is a diagonal matrix whose diagonal elements represent the singular values of $\mathbf{A}$, i.e.,

$$\boldsymbol{\Sigma}=\mathrm{diag}(\sigma_1,\sigma_2,\ldots,\sigma_N) \tag{7}$$

and $\sigma_1\ge\sigma_2\ge\cdots\ge\sigma_N\ge0$ (Trefethen and Bau, 1997). Let the rank of $\mathbf{A}$ be $r\le N$. Hence, $\sigma_{r+1}=\sigma_{r+2}=\cdots=\sigma_N=0$ and equation 6 can be rewritten as

$$\mathbf{A}=\sum_{k=1}^{r}\sigma_k\mathbf{u}_k\mathbf{v}_k^*=\sum_{k=1}^{r}\mathbf{f}_k\mathbf{g}_k^*, \tag{8}$$

where $\mathbf{u}_k$ and $\mathbf{v}_k$ represent the kth column vectors of $\mathbf{U}$ and $\mathbf{V}$, respectively, and $\mathbf{f}_k=\sqrt{\sigma_k}\mathbf{u}_k$ and $\mathbf{g}_k=\sqrt{\sigma_k}\mathbf{v}_k$. Equation 8 suggests that a 2D complex-valued FIR digital filter can be implemented using r parallel 2D subfilters where each 2D subfilter is composed of a cascade of two N-length 1D complex-valued FIR digital filters. These 1D filters have FIR impulse responses given by $f_k(n_1)$ and $g_k(n_2)$. Figure 1 demonstrates the SVD-based implementation structure for the (extrapolation) filtering process where the implementation cost depends on the value of rank r. For a complete representation, the rank r is always equal to $(N+1)/2$ in the case of quadrantally symmetric impulse responses.

SVD implementation of 2D extrapolation FIR filters

For the analysis given below, we will follow Zhu et al. (1999). Define $\mathbf{J}$ to be an $(N-1)/2\times(N-1)/2$ contra-identity matrix where the contra-diagonal elements are equal to 1 and the remaining elements are zeros (N is an odd positive integer). That is,

$$\mathbf{J}=\begin{bmatrix}0 & & 1\\ & \iddots & \\ 1 & & 0\end{bmatrix}. \tag{9}$$

Because $\mathbf{A}\in\mathbb{C}^{N\times N}$ possesses quadrantal symmetry, then $\mathbf{A}$ can be written as

$$\mathbf{A}=\begin{bmatrix}\mathbf{A}_1 & \mathbf{a}_1 & \mathbf{A}_1\mathbf{J}\\ \mathbf{a}_2^* & c & \mathbf{a}_2^*\mathbf{J}\\ \mathbf{J}\mathbf{A}_1 & \mathbf{J}\mathbf{a}_1 & \mathbf{J}\mathbf{A}_1\mathbf{J}\end{bmatrix}, \tag{10}$$

where $\mathbf{A}_1$ is an $(N-1)/2\times(N-1)/2$ matrix, $\mathbf{a}_1$ and $\mathbf{a}_2$ are $(N-1)/2$D column vectors, and c is a complex scalar. The matrix $\mathbf{Q}\in\mathbb{C}^{N\times N}$ given by

$$\mathbf{Q}=\frac{1}{2}\begin{bmatrix}\mathbf{I}+j\mathbf{I} & \mathbf{0} & \mathbf{J}+j\mathbf{J}\\ \mathbf{0} & \sqrt{2}+j\sqrt{2} & \mathbf{0}\\ \mathbf{I}+j\mathbf{I} & \mathbf{0} & -\mathbf{J}-j\mathbf{J}\end{bmatrix} \tag{11}$$

is a unitary matrix where $j=\sqrt{-1}$, $\mathbf{I}$ is the identity matrix with the same dimension of $\mathbf{J}$, and $\mathbf{0}$ is a row/column vector of dimension $(N-1)/2$. A unitary matrix $\mathbf{B}\in\mathbb{C}^{N\times N}$, which is mathematically similar to $\mathbf{A}$, exists and is given by

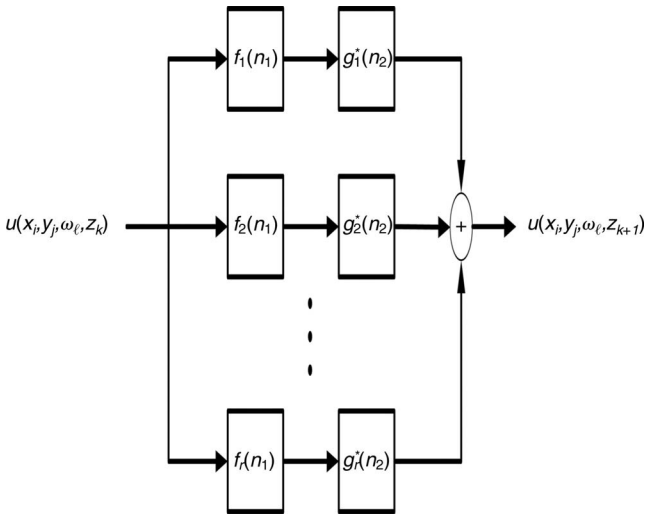

Figure 1. SVD-based implementation structure for a predesigned 2D complex-valued extrapolation FIR digital filter. Each branch represents a 2D subfilter composed of two cascaded 1D extrapolation FIR digital filters.

$$\mathbf{B} = \mathbf{Q}\mathbf{A}\mathbf{Q}^* \tag{12}$$

$$= \begin{bmatrix} \mathbf{A}_1 + \mathbf{J}\mathbf{A}_1\mathbf{J} & \frac{\sqrt{2}}{2}\mathbf{a}_1 + \frac{\sqrt{2}}{2}\mathbf{J}\mathbf{a}_1 & \mathbf{0} \\ \sqrt{2}\mathbf{a}_2^* & 2c & \mathbf{0} \\ \mathbf{0} & \mathbf{0} & \mathbf{0} \end{bmatrix} \tag{13}$$

$$= \begin{bmatrix} \mathbf{B}_1 & \mathbf{0} \\ \mathbf{0} & \mathbf{0} \end{bmatrix}, \tag{14}$$

where $\mathbf{B}_1$ is an $(N+1)/2 \times (N+1)/2$ matrix. Note that $\mathbf{A}^*\mathbf{A}$ is also unitary, which is similar to $\mathbf{B}^*\mathbf{B}$ with respect to $\mathbf{Q}$. This implies that $\mathbf{A}^*\mathbf{A}$ and $\mathbf{B}^*\mathbf{B}$ have the same eigenvalues and, consequently, the same singular values, i.e., the matrices $\mathbf{A}$ and $\mathbf{B}$ are unitary equivalent (Trefethen and Bau, 1997). Now, let the SVD of $\mathbf{B}$ be given by

$$\mathbf{B} = \mathbf{U}_\mathbf{B}\mathbf{\Sigma}_\mathbf{B}\mathbf{V}_\mathbf{B}^*, \tag{15}$$

where $\mathbf{U}_\mathbf{B}$ and $\mathbf{V}_\mathbf{B}$ are unitary and $\mathbf{\Sigma}_\mathbf{B}$ is a diagonal matrix with singular values in decreasing order. From equation 14, we can rewrite equation 15 as

$$\mathbf{B} = \begin{bmatrix} \mathbf{U}_1 & \mathbf{0} \\ \mathbf{0} & \mathbf{0} \end{bmatrix} \begin{bmatrix} \mathbf{\Sigma}_1 & \mathbf{0} \\ \mathbf{0} & \mathbf{0} \end{bmatrix} \begin{bmatrix} \mathbf{V}_1 & \mathbf{0} \\ \mathbf{0} & \mathbf{0} \end{bmatrix}^* \tag{16}$$

and this implies that we can determine the SVD of $\mathbf{B}$, by only computing the SVD of

$$\mathbf{B}_1 = \mathbf{U}_1\mathbf{\Sigma}_1\mathbf{V}_1^* \tag{17}$$

$$= \begin{bmatrix} \mathbf{U}_{11} & \mathbf{b}_1 \\ \mathbf{b}_2^* & U_0 \end{bmatrix} \begin{bmatrix} \mathbf{\Sigma}_{11} & \mathbf{0} \\ \mathbf{0} & \Sigma_0 \end{bmatrix} \begin{bmatrix} \mathbf{V}_{11} & \mathbf{c}_1 \\ \mathbf{c}_2^* & V_0 \end{bmatrix}^*. \tag{18}$$

Thus, $\mathbf{A}$ can be expressed as:

$$\mathbf{A} = \mathbf{Q}^*\mathbf{B}\mathbf{Q} \tag{19}$$

$$= \mathbf{Q}^*\mathbf{U}_\mathbf{B}\mathbf{\Sigma}_\mathbf{B}\mathbf{V}_\mathbf{B}^*\mathbf{Q}, \tag{20}$$

$$= \hat{\mathbf{U}}\mathbf{\Sigma}_\mathbf{B}\hat{\mathbf{V}}^* \tag{21}$$

where

$$\hat{\mathbf{U}} = \mathbf{Q}^*\mathbf{U}_\mathbf{B} \tag{22}$$

$$= \frac{1}{2}\begin{bmatrix} (\mathbf{I} - j\mathbf{I})\mathbf{U}_{11} & (\mathbf{I} - j\mathbf{I})\mathbf{b}_1 & \mathbf{0} \\ (\sqrt{2} - j\sqrt{2})\mathbf{b}_2^* & (\sqrt{2} - j\sqrt{2})U_0 & \mathbf{0} \\ (\mathbf{J} - j\mathbf{J})\mathbf{U}_{11} & (\mathbf{J} - j\mathbf{J})\mathbf{b}_1 & \mathbf{0} \end{bmatrix} \tag{23}$$

and

$$\hat{\mathbf{V}} = \mathbf{Q}^*\mathbf{V}_\mathbf{B} \tag{24}$$

$$= \frac{1}{2}\begin{bmatrix} (\mathbf{I} - j\mathbf{I})\mathbf{V}_{11} & (\mathbf{I} - j\mathbf{I})\mathbf{c}_1 & \mathbf{0} \\ (\sqrt{2} - j\sqrt{2})\mathbf{c}_2^* & (\sqrt{2} - j\sqrt{2})V_0 & \mathbf{0} \\ (\mathbf{J} - j\mathbf{J})\mathbf{V}_{11} & (\mathbf{J} - j\mathbf{J})\mathbf{c}_1 & \mathbf{0} \end{bmatrix}. \tag{25}$$

As expected, only the first $(N+1)/2$ columns of equation 23 and equation 25 are nonzero and they are symmetric. Because $\hat{\mathbf{U}}$ and $\hat{\mathbf{V}}$ are unitary and $\mathbf{A}$ and $\mathbf{B}$ have identical singular values, equation 21 gives an SVD of $\mathbf{A}$. In other words, the SVD of $\mathbf{A}$ can be represented based on equation 21, where the $\mathbf{u}_k$'s and $\mathbf{v}_k$'s in equation 8 are replaced with the first $(N+1)/2$ columns of $\hat{\mathbf{U}}$ ($\hat{\mathbf{u}}_k$'s) and $\hat{\mathbf{V}}$ ($\hat{\mathbf{v}}_k$'s), respectively. By doing so, the SVD computations are much simplified and result in less SVD numerical errors.

We now want to discard insignificant singular values and, therefore, reduce the number of parallel sections required to implement our 2D extrapolation FIR filters, that is, we want to approximate $\mathbf{A}$ by

$$\mathbf{A}_K = \sum_{k=1}^{K} \sigma_k \hat{\mathbf{u}}_k \hat{\mathbf{v}}_k^* = \sum_{k=1}^{K} \hat{\mathbf{f}}_k \hat{\mathbf{g}}_k^*, \tag{26}$$

where $K < (N+1)/2$ (K is the number of used parallel sections). In this case, the number of parallel sections in Figure 1 is reduced and this results in significant savings in terms of the computational complexity for obtaining a final 3D image, whereas according to equation 23 and equation 25 we guarantee the even symmetry of the 1D constituent filters to result in an overall desired wavenumber response. Clearly, because the 1D subfilters are of even symmetry, the number of multiplications per output sample required to implement the 2D complex-valued extrapolation FIR filter using the SVD implementation scheme is $K(N+1)$, where $K < (N+1)/2$. We will save in the number of multiplications per output sample when compared to extrapolation performed via direct convolution taking into consideration that such FIR filters are of quadrantal symmetry as far as

$$K(N+1) < \frac{(N+1)^2}{4}. \tag{27}$$

Similarly, the number of additions per output sample based on the proposed SVD scheme is $2K(N-1)$ because we have K parallel sections and each section is composed of two 1D, even symmetrical FIR filters. The savings in this case are significant compared with the number of additions per output sample when using true 2D convolution (no advantage for the quadrantal symmetry with respect to the number of additions per output sample).

ERROR ANALYSIS

In wavefield extrapolation, the magnitude and phase responses must satisfy certain conditions as described by Thorbecke (1997) and Mousa et al. (2005). So, it is important to quantify the error because of the reduction of the number of parallel sections used to implement our extrapolation FIR digital filters via the SVD method given in equation 26, i.e., via discarded singular values. The following analysis states an upper bound for the SVD implementation of such filtering application with respect to the matrix ℓ_2-norm and the

Frobenius norms of matrices. The error in the wavenumber response of the implemented filter, which is caused by neglecting $((N+1)/2 - K)$ smallest singular values, can be written as

$$\begin{aligned} E(k_x,k_y) &= H(k_x,k_y) - H_K(k_x,k_y) \\ &= \sum_{n_2=-(N-1)/2}^{(N-1)/2} \sum_{n_1=-(N-1)/2}^{(N-1)/2} e[n_1,n_2] e^{-j(k_x n_1 + k_y n_2)} \\ &= \mathbf{\Psi}^*(k_x)\mathbf{E}\mathbf{\Psi}(k_y), \end{aligned} \tag{28}$$

where $H(k_x,k_y)$ is the wavenumber response of the predesigned extrapolation filter, $H_K(k_x,k_y)$ is the wavenumber response of $\mathbf{A}_K = \{h_K[n_1,n_2]\}$ for $|n_1,n_2| \le (N-1)/2$ (see equation 26), $e[n_1,n_2]$ is the error in the FIR impulse response for all values of n_1 and n_2, i.e.,

$$e[n_1,n_2] = h[n_1,n_2] - h_K[n_1,n_2] \tag{29}$$

and $\mathbf{E} = \{e(n_1,n_2)\}$ is its impulse response error matrix, and

$$\mathbf{\Psi}(k_x) = \begin{bmatrix} e^{-jk_x(N-1)/2} \\ \vdots \\ e^{-jk_x} \\ 1 \\ e^{jk_x} \\ \vdots \\ e^{jk_x(N-1)/2} \end{bmatrix} \tag{30}$$

and similarly,

$$\mathbf{\Psi}(k_y) = [e^{-jk_y(N-1)/2},\cdots,e^{-jk_y},1,e^{jk_y},\cdots,e^{jk_y(N-1)/2}]^*. \tag{31}$$

We can now rewrite $\mathbf{E}$ as:

$$\begin{aligned} \mathbf{E} = \mathbf{A} - \mathbf{A}_K &= \sum_{k=1}^{(N+1)/2} \sigma_k \hat{\mathbf{u}}_k \hat{\mathbf{v}}_k^* - \sum_{k=1}^{K} \sigma_k \hat{\mathbf{u}}_k \hat{\mathbf{v}}_k^* \\ &= \sum_{k=K+1}^{(N+1)/2} \sigma_k \hat{\mathbf{u}}_k \hat{\mathbf{v}}_k^* = \mathbf{U}_\mathbf{E}\mathbf{\Sigma}_\mathbf{E}\mathbf{V}_\mathbf{E}^*, \end{aligned} \tag{32}$$

where $\mathbf{\Sigma}_E = \mathrm{diag}(\sigma_{K+1},\ldots,\sigma_{(N+1)/2},0,\ldots,0)$ and $\mathbf{U}_\mathbf{E}$ and $\mathbf{V}_\mathbf{E}$ are complex-valued unitary matrices of dimension $N \times N$. By substituting equation 32 for equation 28 and taking the absolute value of the result, we obtain

$$|E(k_x,k_y)| = |\mathbf{\Psi}^*(k_x)\mathbf{U}_\mathbf{E}\mathbf{\Sigma}_\mathbf{E}\mathbf{V}_\mathbf{E}^*\mathbf{\Psi}(k_y)|. \tag{33}$$

Now, using the Cauchy-Schwartz inequality and because $\mathbf{U}_\mathbf{E}$ and $\mathbf{V}_\mathbf{E}$ are unitary, we can show that the upper bound of the absolute wavenumber response error with respect to the matrix Frobenius norm is:

$$\max_{-\pi \le k_x,k_y \le \pi} |E(k_x,k_y)| \le N \left[\sum_{k=K+1}^{(N+1)/2} \sigma_k^2 \right]^{1/2}. \tag{34}$$

A much tighter bound can be found based on the matrix ℓ_2-norm and is given by

$$\max_{-\pi \le k_x,k_y \le \pi} |E(k_x,k_y)| \le N\sigma_{K+1}. \tag{35}$$

For this application, equations 34 and 35 quantify the magnitude wavenumber response error introduced using the proposed SVD implementation method with $K < (N+1)/2$.

It is difficult, however, to analytically find an upper bound for the error incurred by the phase response of the SVD-implemented extrapolation filter. However, based on empirical results, the circular symmetry of the wavenumber phase response is always achieved when discarding insignificant singular values. As we are going to show in simulations, one possible way to relate the phase error with the singular values is by plotting the relationship between the number of parallel sections used, the total energy used per number of used parallel sections, and the corresponding phase response error.

SIMULATION RESULTS

The following simulations are divided into two subsections. The first subsection deals with the accuracy of implementing 2D complex-valued extrapolation FIR filters using the SVD implementation method presented previously and given by equation 26. Also, this implementation is compared with the original and the improved McClellan transformation implementation schemes (Hale, 1991a) in terms of the implemented filters' wavenumber responses, the passband and stopband maximum and mean absolute wavenumber errors, and the computational cost. The second subsection is concerned with applying the implemented 2D complex-valued extrapolation FIR filters using our proposed SVD implementation scheme for seismic impulse response wavefields and again comparing with those extrapolated sections using the original and the improved McClellan transformations (Hale, 1991a).

Accuracy of the 2D extrapolation FIR digital filters implemented via SVD

The main focus of this section is to subjectively and objectively evaluate our proposed implementation scheme for the extrapolation filters and to compare it with the benchmark implementations used in practice in terms of the wavenumber responses and the computational complexity. For this, a 25×25 complex-valued extrapolation FIR filter was designed using the modified projections onto convex sets (POCS) method (Mousa et al., 2005, 2006) for $\Delta z = 2$ m, $\Delta x = \Delta y = 10$ m, $\Delta t = 0.004$ s, $\omega = 0.4\pi$ rad/s, and a velocity $c_o = 1000$ m/s, to give a normalized cutoff wavenumber of $k_{c_p} = 0.25$.

Implementation of 2D extrapolation FIR digital filters via SVD

Figures 2a and 3a, respectively, show the magnitude response and the phase response in the wavenumber domain of the predesigned 2D extrapolation FIR filter with the above-mentioned parameters. The 2D FIR filter impulse response matrix is then transformed to be in the form of equation 14 and then decomposed to give the resultant $\mathbf{B}_1$ matrix based on equation 16. The rank of the impulse response matrix of this filter is of full rank, i.e., $\mathrm{rank}(\mathbf{B}_1) = 13$, that is, the number of parallel sections that can be used to correctly implement such filters is equal to thirteen sections. However, Figure 4 suggests that we can implement such a filter matrix with a reduced number of parallel sections (see Figure 1) by discarding the insignificant singular values according to equation 26 (where we can see that four or five parallel sections are sufficient to implement our filter). This is because more than 99% of the energy is concentrated in the first four or five singular values according to the singular values displayed in

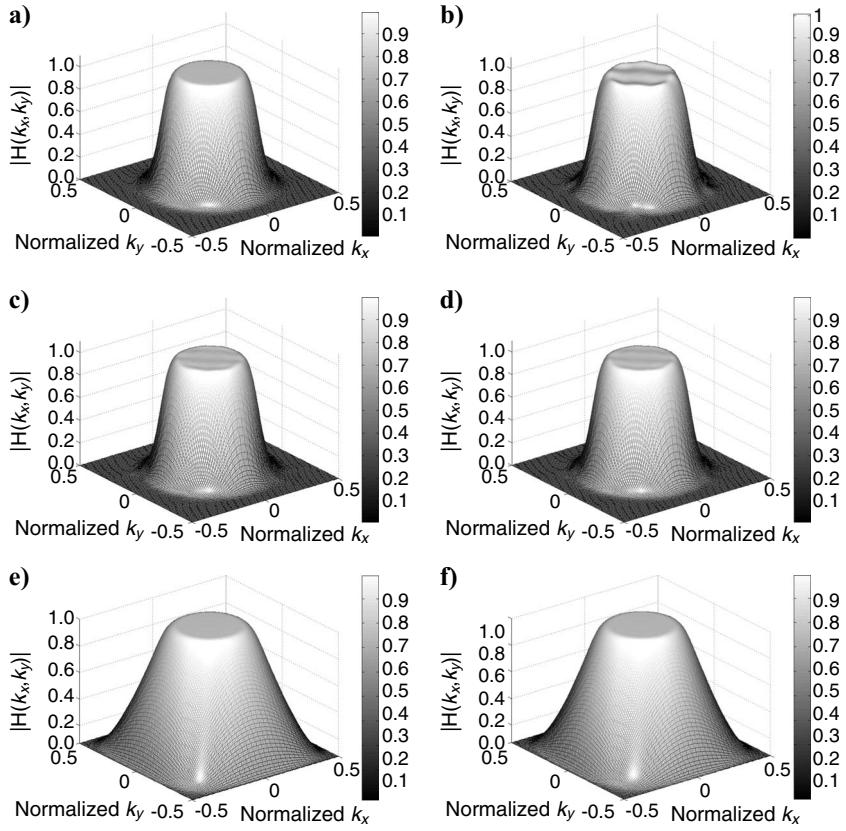

Figure 2. A 25×25 2D extrapolation FIR digital filter (with a normalized wavenumber cutoff $k_{c_p} = 0.25$) showing plots of the magnitude spectrum for the (a) predesigned, (b) SVD implemented with $K = 3$, (c) SVD implemented with $K = 4$, (d) SVD implemented with $K = 5$, (e) original McClellan transformation method, and (f) improved McClellan transformation method.

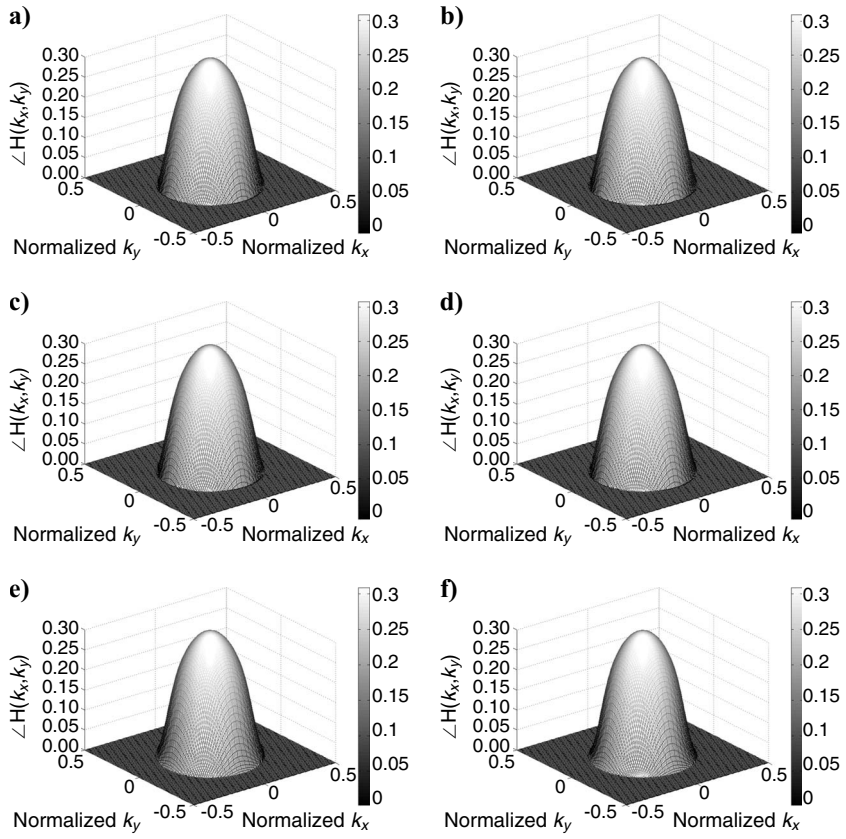

Figure 3. A 25×25 2D extrapolation FIR digital filter (with a normalized wavenumber cutoff $k_{c_p} = 0.25$) showing plots of the passband phase spectrum (in radians) for the (a) predesigned, (b) SVD implemented with $K = 3$, (c) SVD implemented with $K = 4$, (d) SVD implemented with $K = 5$, (e) original McClellan transformation method, and (f) improved McClellan transformation method.

Figure 4. The selection can be quantitatively dependent upon a threshold ϵ in accordance with either equations 35 or 34.

In Figure 5, the passband and stopband maximum absolute wavenumber errors are plotted versus the number of parallel sections used (or the number of used singular values). As expected, both curves are always less than the matrix ℓ_2-norm bound curve as given by equation 35, as well as less than the matrix Frobenius norm bound curve as given by equation 34. Also, we can clearly see that as we use more parallel sections (incorporate more singular values in the approximation), then the approximation error will decrease. However, this will be at the expense of increasing the number of multiplications and additions per output sample. The passband and stopband errors when using five parallel sections are less by 15 dB on average when compared to the errors introduced through using four parallel sections. Now, to quantify the passband phase error incurred because of the use of equation 26, we calculated the maximum as well as the root-mean-squared (RMS) passband phase errors (for different number of used parallel sections and total used energy per implementation) for our SVD-implemented filter as shown in Figure 6. It is evident from this figure that both errors will approach zero as we use more parallel sections. For $K = 5$, the maximum and RMS passband phase errors are almost identical and close to zero. This also agrees with Figure 4 where it is shown that most of the energy (more than 99%) is concentrated within the first five singular values.

Furthermore, the magnitude and the phase spectrum responses are of circular symmetry. This can be seen more clearly with plots that are given for the magnitude and phase spectra using the SVD implementation schemes in Figure 2b for $K = 3$, c for $K = 4$, and d for $K = 5$, and Figure 3b for $K = 3$, c for $K = 4$, and d for $K = 5$, respectively. For the SVD implementations with $K = 3$, $K = 4$, and $K = 5$, the phase response plots indicate no deviation in the circularity of the phase responses. On the other hand, the magnitude response in Figure 2d for $K = 5$ is subjectively better (circular symmetry) when compared to Figure 2b (for $K = 3$) and c (for $K = 4$). Hence, overall, using five parallel sections in this case is the best choice among others. Therefore, we implemented our 2D extrapolation FIR filters with only five parallel sections out of thirteen.

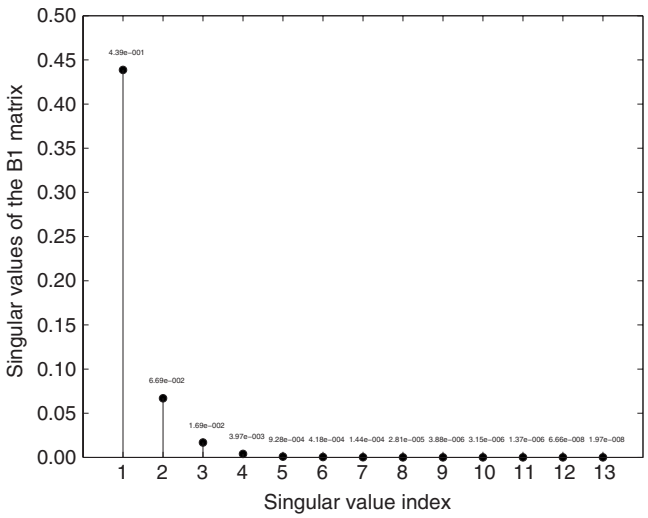

Figure 4. Singular values of the matrix $\mathbf{B}_1$ (see equation 18) for the predesigned 25×25 2D extrapolation FIR digital filter.

Comparisons with the McClellan transformations

To compare the SVD implementation with the standard implementations used for this application, a 1D complex-valued extrapolation FIR filter was predesigned using the method of modified POCS (Mousa et al., 2005) with the same filter parameters described earlier. This 1D filter is then transformed into a 2D filter by the McClellan transformation and its improved version (Hale, 1991a). Figure 2e and Figure 3e show plots of McClellan transformed filter magnitude and phase response, whereas Figure 2f and Figure 3f show the magnitude and phase response plots for the improved McClellan transformed filter. In both cases, the circularity of the magnitude and the phase responses for both McClellan transformation results deteriorate rapidly as k_x and k_y increase, although the improved

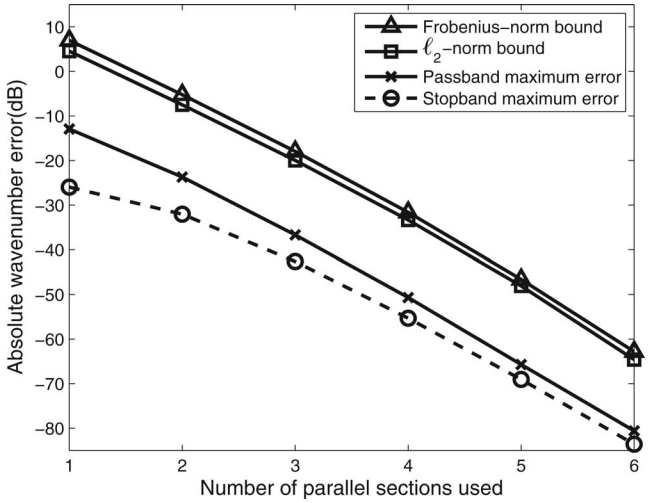

Figure 5. Maximum absolute wavenumber error bounds and within the passband and the stopband for the SVD-implemented predesigned 25×25 2D extrapolation FIR digital filter with respect to the number of parallel sections used (i.e., the number of singular values).

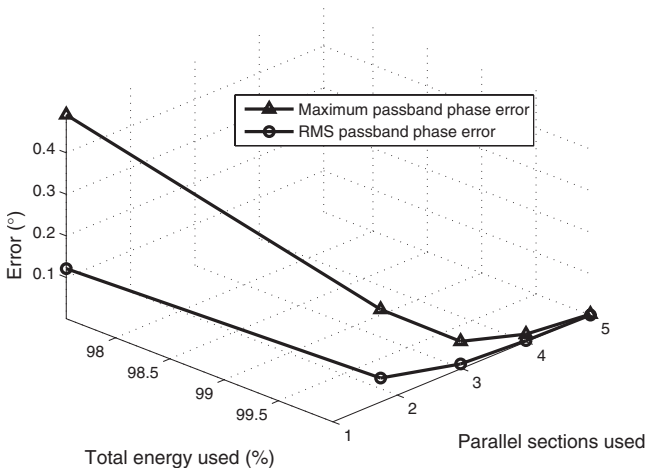

Figure 6. Maximum and root-mean-squared phase errors within the passband for the SVD-implemented predesigned 25×25 2D extrapolation FIR digital filter with respect to the number of parallel sections used (i.e., the number of singular values) as well as the total used energy.

results possess less errors when compared to the original McClellan transformation. This is unlike our proposed SVD implementation method where we do obtain an almost perfect circular symmetry in the magnitude and the phase responses as seen, for example, in Figure 2d and Figure 3d.

Table 1 compares the three implementations, namely, the McClellan method, the improved McClellan method, and our SVD method with $K = 5$ in terms of the passband and stopband maximum and mean absolute wavenumber errors. As we can see from Table 1, the SVD implementation with five parallel sections presents the implementation with the lowest significant passband as well as stopband maximum and mean absolute wavenumber errors and, therefore, outperforms both McClellan implementations.

Finally, Table 2 compares the number of multiplications and additions per output sample between various implementation schemes, including our proposed SVD method. It is clear from both tables that the original McClellan transformation is the cheapest among all of these schemes, including our proposed SVD ($K = 5$) technique. In terms of the number of multiplications per output sample, the proposed SVD ($K = 5$) technique, however, is more economical than the true 2D convolution with quadrantal symmetry (saved more than 23%). Also, in terms of the number of additions per output sample, our proposed SVD ($K = 5$) method saved about 62% when compared with the 2D direct convolution. It is worth mentioning that although our proposed SVD implementation method (depending on K) might be more expensive than the McClellan transformations, it results in much better circularly symmetric magnitude and phase responses, and comes with insignificant wavenumber errors. This consequently results in obtaining superior 3D migration results when compared to 3D migration based on both McClellan transformations as we shall see in the next subsection.

Table 1. Comparison of the mean and maximum absolute errors within passband and stopband wavenumber responses between the predesigned 2D extrapolation FIR filter and its implemented version using the original McClellan transformation, the improved McClellan transformation, and our proposed SVD implementation with $N = 25$.

Method	$\lvert E(k_x,k_y)\rvert$	Passband	Stopband
Original	Mean	374.6E − 3	100.6E − 3
McClellan	Max	2004.5E − 3	502.2E − 3
Improved	Mean	374.4E − 3	94.2E − 3
McClellan	Max	2004.6E − 3	463.2E − 3
SVD implementation	Mean	0.038E − 3	0.011E − 3
with $K = 5$	Max	0.518E − 3	0.353E − 3

3D seismic extrapolation impulse response tests

To test our SVD-implemented extrapolation filters for 3D seismic extrapolation impulse responses, a synthetic seismic volume was created. It is basically composed of zero amplitude traces containing one zero-phase Ricker wavelet centered at 0.512 second and is located at $x = y = 0$ seismic trace. In this experiment, a set of 25×25 2D extrapolation FIR digital filters were designed using the method of modified POCS (Mousa et al., 2005, 2009) and stored with the same filter parameters mentioned earlier. The range of inline and crossline sections was 1100 meters. Also, for this experiment, the maximum normalized angular frequency used was 0.72π rad/s. These 2D designed filters were used to perform 3D wavefield extrapolation based on true 2D convolution (taking into account the quadrantal symmetry of such filters) and based on our SVD-derived implementation scheme given by equation 26 with $K = 3$, 4, and 5 for the above-mentioned predesigned filters. A 2D slice of the extrapolated volume at $z = 220$ m (which corresponds to an angle of 65°) as well as at $x = 0$ and $y = 0$ all are shown in Figure 7 using true direct convolution, and using our SVD implementation scheme with $K = 3$ (Figure 8), $K = 4$ (Figure 9), and $K = 5$ (Figure 10). Subjectively, the slices of the extrapolated volume via SVD implementation with $K = 5$ in Figure 10 is the best among the other two extrapolated wavefields with the SVD implementation with $K = 3$ (see Figure 8) and with $K = 4$ (see Figure 9).

The same input seismic volume described above was extrapolated using the McClellan and the improved McClellan transformation schemes. A set of 25-length 1D extrapolation FIR digital filters were predesigned and stored to perform such an experiment again with the same filter parameters stated earlier. Figures 11 and 12 show the same 2D slices of the 3D extrapolated sections at $z = 220$ m, $x = 0$, and $y = 0$. Although the improved McClellan slice given in Figure 12 has a better response when compared to the extrapolated section slices in Figure 11 using the original McClellan method, both methods result in poor extrapolated images when compared to the SVD-extrapolated depth section with $K = 5$ (Figure 10). The differences can be seen clearly where the McClellan transformation migration

Table 2. Comparison between the number of multiplications and additions per output sample required to implement a 2D complex-valued extrapolation FIR filter using the direct 2D convolution with quadrantal symmetry, the original McClellan transformation, the improved McClellan transformation, and our proposed SVD implementation with $N = 25$. Note that the savings are calculated with respect to the 2D convolution with symmetry cost.

Method	Multiplications per output sample	Savings	Additions per output sample	Savings
2D convolution with symmetry	$\left(\frac{N+1}{2}\right)^2 = 169$	—	$N^2 - 1 = 624$	—
McClellan	$5\left(\frac{N-1}{2}\right) + 1 = 61$	63.91%	$9\left(\frac{N-1}{2}\right) - 2 = 106$	83.01%
Improved McClellan	$8\left(\frac{N-1}{2}\right) + 1 = 97$	42.6%	$12\left(\frac{N-1}{2}\right) - 2 = 142$	77.24%
SVD ($K = 5$)	$K(N+1) = 130$	23.08%	$2K(N-1) = 240$	61.54%

results are not perfectly symmetrical circles and they possess more dispersion noise. This is in agreement with the simulation results shown in the previous subsection.

DISCUSSION

All the predesigned 2D extrapolation FIR digital filters were designed using the modified POCS method (Mousa et al., 2005, 2006, 2009). However, this does not prevent the use of 2D extrapolation FIR digital filters designed using any 2D filter design method such as those reported by Thorbecke et al. (2004) or by Soubaras (1996). Furthermore, the selection of the appropriate number of parallel sections, namely K, will be the choice of the designer. For example, the designer can automate the selection by:

- considering either equation 35 or equation 34, which deal with absolute wavenumber error bounds;
- the ratio between the maximum and RMS passband phase error; and finally
- equation 27, which gives the bound for the maximum number of multiplications per output sample compared with direct convolution.

It is worth mentioning that the error introduced by the SVD implementation approach is an additional error to the error incurred because of the approximation of the ideal extrapolators with 2D FIR

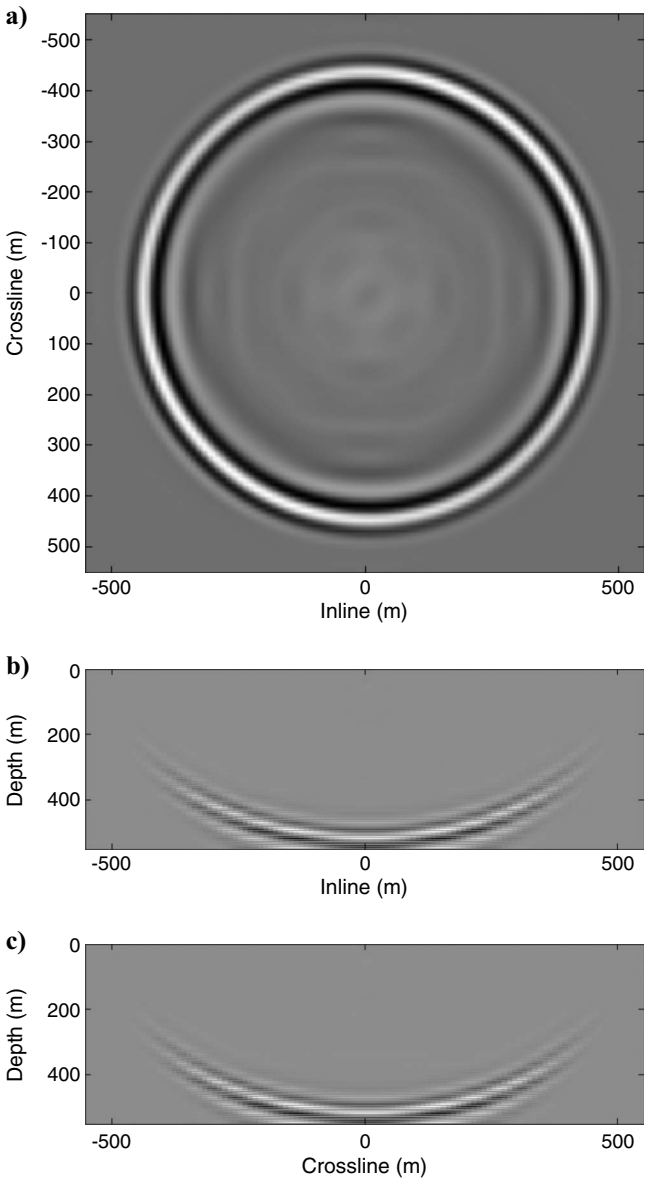

Figure 7. Seismic extrapolation impulse response 2D slices in 3D at (a) depth $z = 220$ m, which corresponds to 65° (b) $y = 0$ m, and (c) $x = 0$ m using direct convolution.

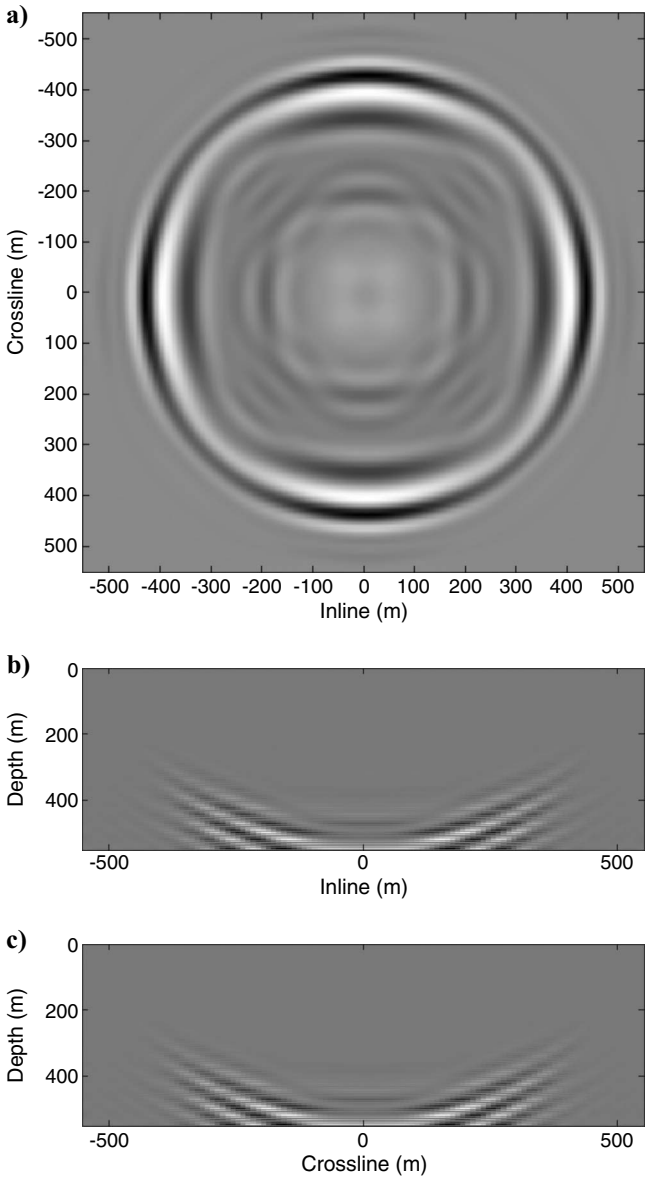

Figure 8. Seismic extrapolation impulse response 2D slices in 3D at (a) depth $z = 220$ m, which corresponds to 65°, (b) $y = 0$ m, and (c) $x = 0$ m using our proposed SVD implementation scheme with $K = 3$.

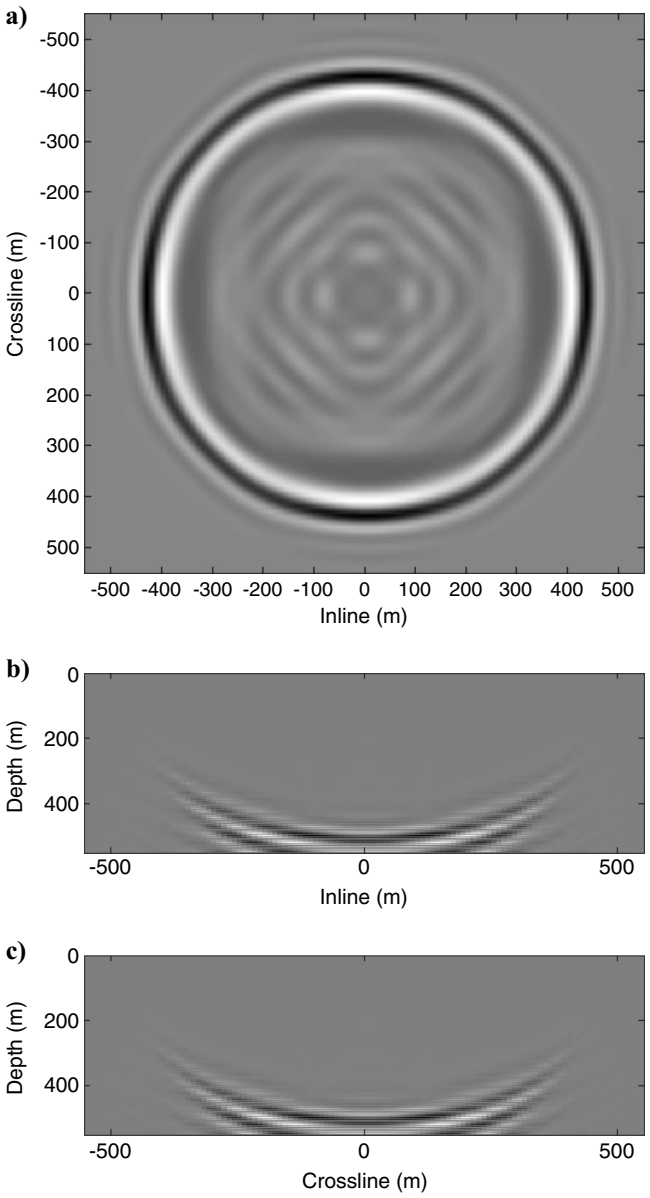

Figure 9. Seismic extrapolation impulse response 2D slices in 3D at (a) depth $z = 220$ m, which corresponds to 65°, (b) $y = 0$ m, and (c) $x = 0$ m using our proposed SVD implementation scheme with $K = 4$.

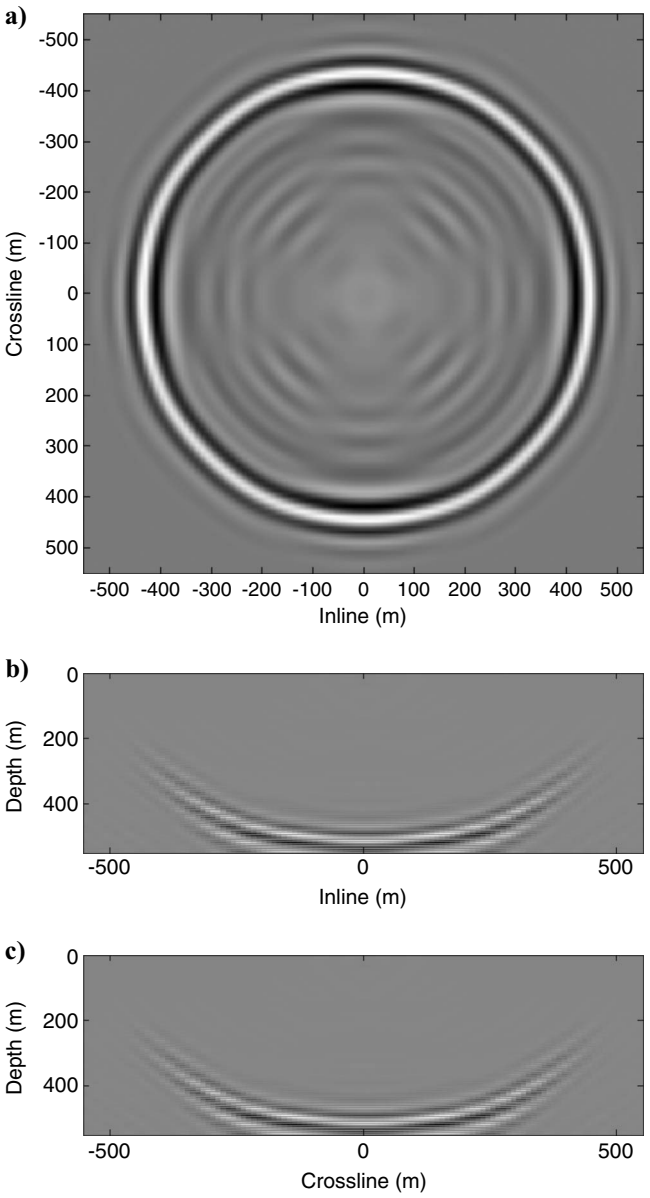

Figure 10. Seismic extrapolation impulse response 2D slices in 3D at (a) depth $z = 220$ m, which corresponds to 65°, (b) $y = 0$ m, and (c) $x = 0$ m using our proposed SVD implementation scheme with $K = 5$.

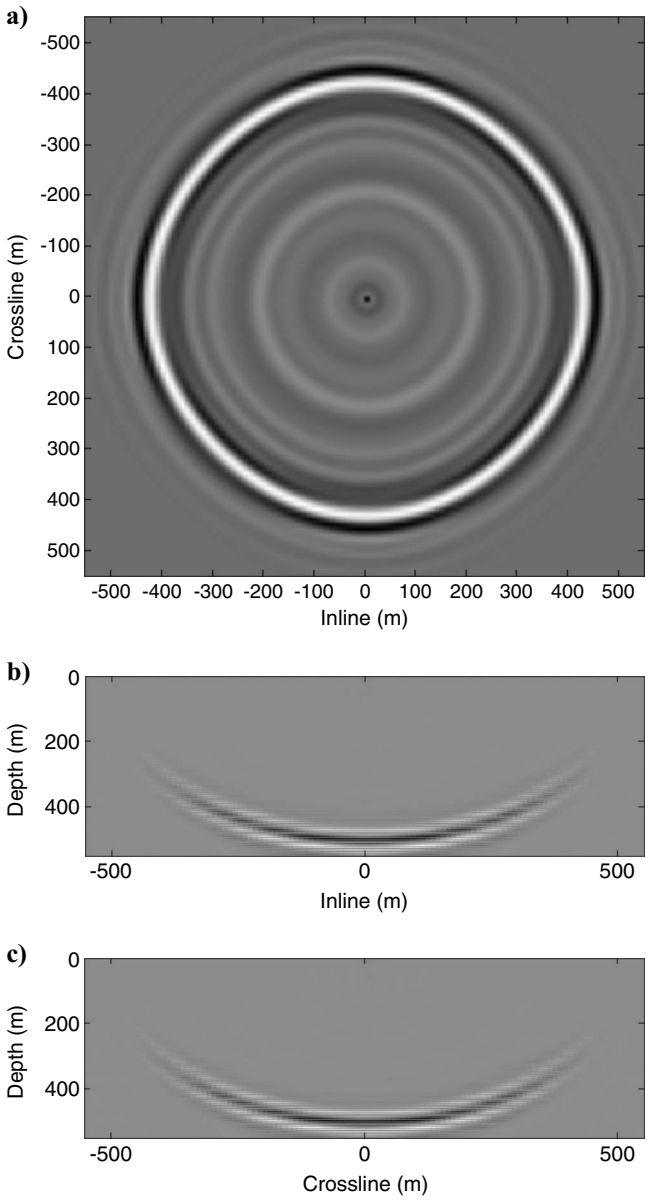

Figure 11. Seismic extrapolation impulse response 2D slices in 3D at (a) depth $z = 220$ m, which corresponds to 65°, (b) $y = 0$ m, and (c) $x = 0$ m using the original McClellan transformation method.

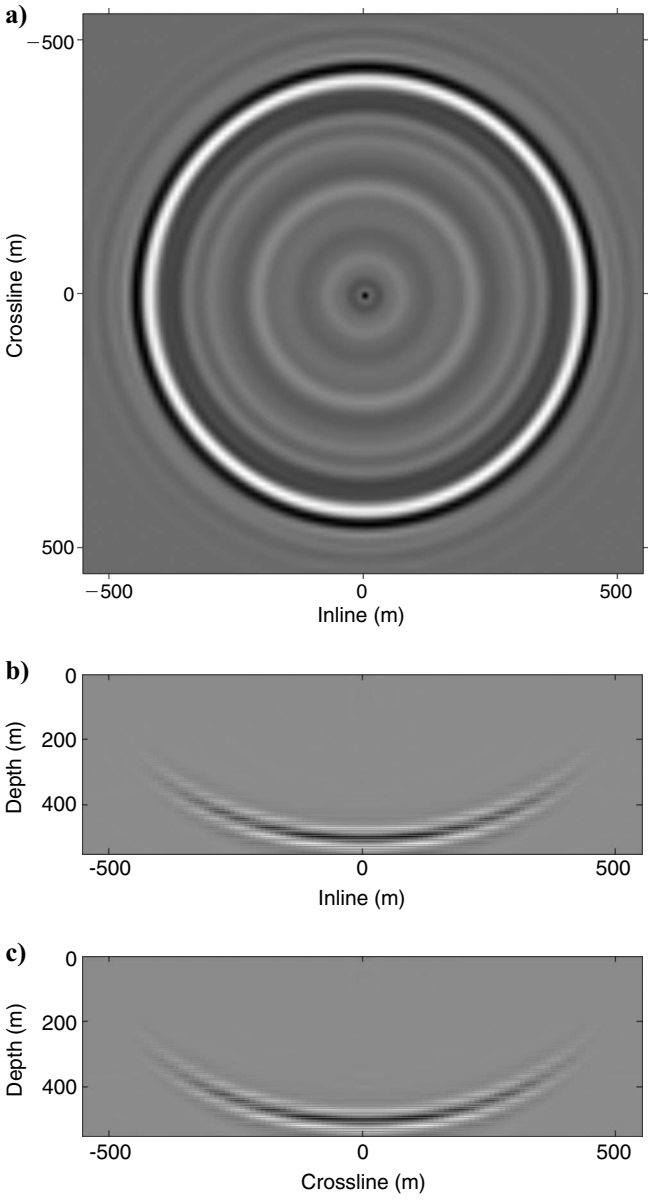

Figure 12. Seismic extrapolation impulse response 2D slices in 3D at (a) depth $z = 220$ m, which corresponds to 65°, (b) $y = 0$ m, and (c) $x = 0$ m using the improved McClellan transformation method.

extrapolation filter coefficients and, hence, the extrapolation of synthetics also will help in the selection of the appropriate K value as well as assist in analyzing the introduced error because of the SVD implementation. Finally, although the extrapolation impulse response example given in this paper was basically for poststack migration, we can use our proposed implementation scheme for prestack migration of rectangularly sampled data sets. If the prestacked data are irregularly sampled (as usually is), it will then be required to rectangularly resample such data prior to applying our proposed SVD implementation.

CONCLUSION

We have adapted the work performed by Zhu et al. (1999) to the application of SVD for implementing 2D quadrantally symmetric complex-valued extrapolation FIR digital filters that are used for applying 3D wavefield extrapolation. To simplify the SVD computations for such an FIR filter impulse response structure, we applied a special matrix transformation on the extrapolation FIR filter impulse responses where the wavenumber phase response is guaranteed to be retained. For the examples given in this paper, the SVD implementation saved more than 23% of the number of multiplications per output sample when compared to direct implementation with symmetry via true 2D convolution. Also, the SVD implementation saved approximately 62% of the number of additions per output sample when compared to direct implementation with symmetry via true 2D convolution. We can obtain similar savings depending on the size of our original 2D operator. Wavenumber magnitude and phase responses possess circular symmetry unlike extrapolation FIR filters implemented with the McClellan and the improved McClellan transformations for such geophysical applications. Finally, we demonstrated our work by applying such SVD-implemented 2D extrapolation FIR filters to test seismic impulse responses. We showed subjectively and objectively that wavefield extrapolation via our proposed SVD implementation scheme is outperforming extrapolation results via the McClellan and the improved McClellan implementations. This was clearly seen in terms of the wavenumber responses, and the maximum and mean passband and stopband absolute wavenumber errors. The SVD approach possesses a bit higher computational cost when compared to the McClellan and the improved McClellan implementations. Having said that, this approach gives us the advantage of obtaining more accurate extrapolated seismic wavefields than those obtained using both implementations and with much lower complexity compared with true 2D convolution.

ACKNOWLEDGMENTS

The authors would like to express their deep appreciation to King Fahd University of Petroleum and Minerals for sponsoring this research work. We also thank Dr. Abdullatif Al-Shuhail, Associate Professor, Earth Sciences Department, King Fahd University of Petroleum & Minerals, for his comments. We finally would like to thank the associate editor and the reviewers for all their valuable comments and suggestions.

REFERENCES

Dudgeon, D. E., and R. M. Mersereau, 1984, Multidimensional digital signal processing: Prentice-Hall.

Hale, D., 1991a, 3-D migration via McClellan transformation: Geophysics, **56**, 1778–1785.

———, 1991b, Stable explicit depth extrapolation of seismic wavefields: Geophysics, **56**, 1770–1777.

Holberg, O., 1988, Towards optimum one-way wave propagation: Geophysical Prospecting, **36**, 99–114.

Karam, L. J., and J. H. McClellan, 1995, Complex Chebyshev approximation for FIR filter design: IEEE Transactions on Circuits and Systems, **42**, 207–216.

———, 1997, Efficient design of digital filters for 2-D and 3-D depth migration: IEEE Transactions on Signal Processing, **45**, 1036–1044.

Kayran, A. H., and R. A. King, 1983, Design of recursive and nonrecursive fan filters with complex transformation: IEEE Transactions on Circuits and Systems, **30**, 849–857.

Lu, W., and A. Antoniou, 1992, Two-dimensional digital filters, 1st ed.: Marcel Dekker Publisher.

Lu, W.-S., H.-P. Wang, and A. Antoniou, 1990, Design of two-dimensional FIR digital filters by using the singular-value decomposition: IEEE Transactions on Signal Processing, **37**, 35–46.

———, 1991, Design of two-dimensional digital filters using singular-value decomposition and balanced approximation method: IEEE Transactions on Signal Processing, **39**, 2253–2262.

McClellan, J., and D. S. K. Chan, 1977, A 2-D, FIR filter structure derived from the Chebyshev recursion: IEEE Transactions on Circuits and Systems, **24**, 372–378.

Mecklenbräuker, W. F., and R. M. Mersereau, 1976, McClellan transformations for two-dimensional digital filtering: I-design: IEEE Transactions on Circuits and Systems, **23**, 405–414.

Mousa, W. A., M. V. D. Baan, S. Boussakta, and D. McLernon, 2009, Designing stable operators for explicit depth extrapolation of 2D & 3D wavefields using projections onto convex sets: Geophysics, **74**, no. 2, S33–S45.

Mousa, W. A., S. Boussakta, M. V. der Baan, and D. C. McLernon, 2006, Designing stable operators for explicit depth extrapolation of 3D wavefields using projections onto convex sets: 76th Annual International Meeting, SEG, Expanded Abstracts, 2589–2593.

Mousa, W. A., D. C. McLernon, S. Boussakta, and M. V. der Baan, 2005, The design of wavefield extrapolators using projections onto convex sets: 75th Annual International Meeting, SEG, Expanded Abstracts, 2037–2040.

Reshef, M., and D. Kessler, 1989, Practical implementation of three-dimensional poststack depth migration: Geophysics, **54**, 309–318.

Soubaras, R., 1996, Explicit 3-D migration using equiripple polynomial expansion and Laplace synthesis: Geophysics, **61**, 1386–1393.

Thorbecke, J., 1997, Common focus point technology: Ph.D. thesis, Delft University of Technology.

Thorbecke, J. W., and A. J. Berkhout, 1994, 3D recursive extrapolation operators: An overview: 64th Annual International Meeting, SEG, Expanded Abstracts, 1262–1265.

Thorbecke, J. W., K. Wapenaar, and G. Swinnen, 2004, Design of one-way wavefield extrapolation operators, using smooth functions in WLSQ optimization: Geophysics, **69**, 1037–1045.

Trefethen, L. N., and D. Bau, 1997, Numerical linear algebra: Society for Industrial and Applied Mathematics.

Yilmaz, ed., 2001, Seismic data analysis: Processing, inversion, and interpretation of seismic data, 2nd ed.: Society of Exploration Geophysicists.

Zhu, W.-P., M. O. Ahmad, and M. N. S. Swamy, 1999, Realization of 2-D linear-phase FIR filters by using the singular valued decomposition: IEEE Transactions on Signal Processing, **47**, 1349–1358.